Scripta Materialia 157 (2018) 49–53

Contents lists available at ScienceDirect

Scripta Materialia

journal homepage: www.elsevier.com/locate/scriptamat

Regular article

Quantifying early stage irradiation damage from nanoindentation pop-in tests☆

K. Jin [a], Y. Xia [b], M. Crespillo [b], H. Xue [b], Y. Zhang [a,b], Y.F. Gao [b,a], H. Bei [a,*]

[a] Materials Science & Technology Division, Oak Ridge National Laboratory, Oak Ridge, TN 37831, USA
[b] Department of Materials Science & Engineering, University of Tennessee, Knoxville, TN 37996, USA

ARTICLE INFO

Article history:
Received 7 April 2018
Received in revised form 20 June 2018
Accepted 24 July 2018
Available online xxxx

Keywords:
Ion irradiation
Nanoindentation
Pop-in
Incipient plasticity

ABSTRACT

Early stage irradiation effects on incipient plasticity are quantitatively investigated in single-crystalline molybdenum using nanoindentation pop-in tests. Defects produced under low-dose ion irradiations, even when they are hardly detected by ion-channeling technique, can significantly reduce the critical stress for the elastic-plastic transition, through acting as heterogeneous dislocation nucleation sources. The density and strength of defects are derived using a unified model convoluting homogeneous and heterogeneous mechanisms. In addition to the increased defect density, defect strength is found to decrease with increasing irradiation dose, suggesting a growth in defect size, which is further evidenced by combined analyses between pop-in and hardness tests.

Quantitative characterization of early stage defect production and evolution in ion-irradiated materials is essential to both fundamental materials science and various application fields [1–3]. For example, it bridges atomistic simulations, which primarily focus on the low dose regime, to the experimentally observed microstructure and property evolution after long-term irradiations [3–5]. In addition, it is required in developing and validating novel design concepts of irradiation-resistant materials that suppress early stage damage accumulation [6, 7].

Nonetheless, quantification of low-dose ion irradiation damage has been a long-standing challenge, mainly attributed to the small defect size and the limited penetration depth. The former leads to difficult statistical analyses in microscopic studies; the latter makes thin film samples required for electrical resistivity measurements [8], which usually brings a tedious or challenging sample preparation process, especially when specific material microstructures and configurations are required.

Pop-in phenomenon refers to the sudden displacement excursion on the load-displacement curves during nanoindentation tests, and arises from the onset of elastic-plastic transition [9–13]. In crystalline materials, pop-in originates from homogeneous dislocation nucleation at the theoretical strength, if no lattice defects are initially present. Pre-existing defects can serve as heterogeneous dislocation nucleation sources that require lower initiation stresses [9, 13], see Fig. 1a; the defect density and strength can both be derived from the cumulative probability distribution of the pop-in loads using a statistical model [9]. Pop-in load is very sensitive to crystal damage, which probably leads to the fact that pop-in has hardly been observed in previous nanoindentation studies on irradiated materials, without quantitative knowledge on how pop-in behavior progresses under irradiations [14, 15].

In this study, we investigate the impact of ion irradiation on the incipient plasticity of single crystalline Molybdenum (Mo), and demonstrate nanoindentation pop-in test as an effective quantification method in studying early stage irradiation damage. Utilizing a statistic model, pop-in tests can quantify not only the density of defect clusters, but also the change in defect strength, which is further correlated to the defect size. Moreover, the damage accumulation is compared with that characterized using ion channeling, a widely used technique for irradiated single-crystals [16].

Pure Mo (99.99% purity) with (100) surface was homogenized at 1600 °C for 4 h under vacuum. The samples were ground and polished using a standard metallographic procedure, and then electro-polished in a solution of 12.5% H_2SO_4 and 87.5% CH_3OH at a DC voltage of 10 V to remove the surface mechanical damage. The samples were irradiated with 10 MeV Ni ions at room temperature, with fluences from 2.5×10^{12} to 1.6×10^{14} cm^{-2} and a constant flux of 3.5×10^{11} cm^{-2} s^{-1} [17]. The profiles of displacement and implanted ions were estimated using SRIM

☆ This manuscript has been authored by UT-Battelle, LLC under Contract No. DE-AC05-00OR22725 with the U.S. Department of Energy. The United States Government retains and the publisher, by accepting the article for publication, acknowledges that the United States Government retains a non-exclusive, paid-up, irrevocable, world-wide license to publish or reproduce the published form of this manuscript, or allow others to do so, for United States Government purposes. The Department of Energy will provide public access to these results of federally sponsored research in accordance with the DOE Public Access Plan (http://energy.gov/downloads/doe-public-access-plan).

* Corresponding author.
E-mail address: hbei1@utk.edu (H. Bei).

https://doi.org/10.1016/j.scriptamat.2018.07.035
1359-6462/

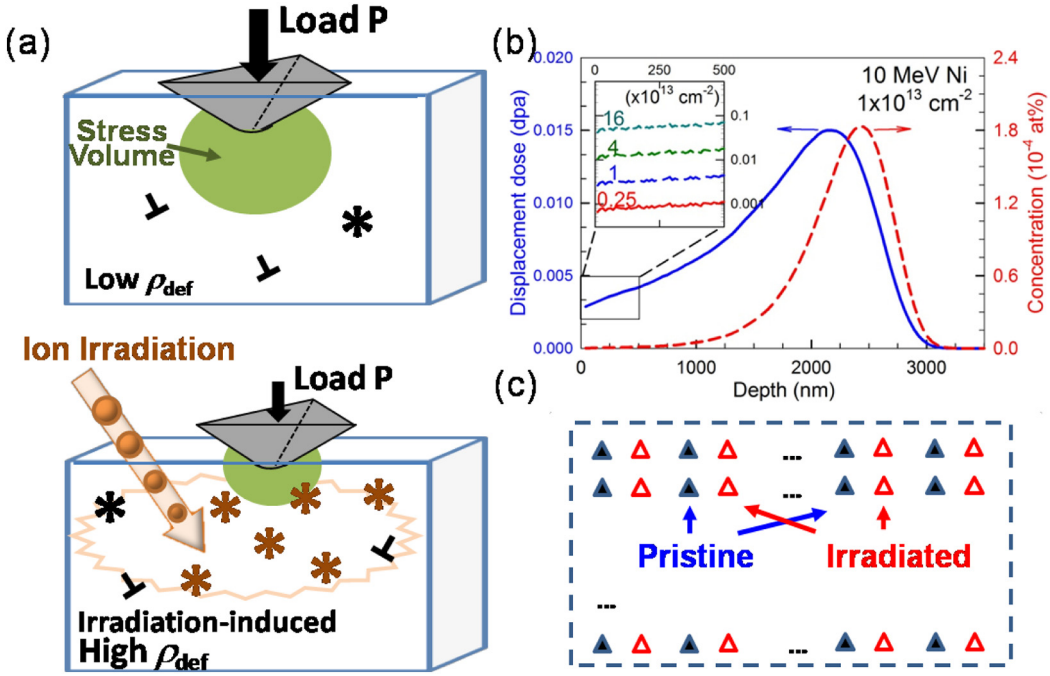

Fig. 1. Illustration of concepts and experiments. (a) Schematic illustration of the dominant mechanisms of nanoindentation pop-in before and after ion irradiations. "⊥" represents the Frank-Read sources, e.g. dislocations, and "*" represents the defect clusters acting as heterogeneous dislocation nucleation cores. (b) SRIM predicted damage and ion profiles after 10 MeV Ni ion irradiations in Mo at the fluence of 1×10^{13} cm^{-2}; the inset is the enlarged depth region of 0–500 nm at all four fluences. (c) The arrangements of indents of nanoindentation tests.

[18] simulation in the Kinchin-Pease mode, assuming a threshold displacement energy of 33 eV [19], as shown in Fig. 1b. The damage peak is located at ~2.2 μm, and the local displacement dose only gradually changes in the surface regime to a relatively small extent (inset of Fig. 1b). Since pop-in occurs within a few tens of nanometers from surface (as will be shown below), the surface dose values, rather than the peak values, are used in the present study, ranging from ~7.5×10^{-4} to 4.8×10^{-2} displacements per atom (dpa). Almost no implanted Ni ions were introduced in the surface region. Ion channeling measurements were performed using 3.5 MeV He ions with a 155° scattering angle [17].

Nanoindentation tests were performed using Nanoindenter XP (Nano Instruments Innovation Center, MTS Corporation, Knoxville, TN), in the same region before and after irradiations in an alternating pattern for each dose as shown in Fig. 1c. A Berkovich triangular pyramid indenter with a blunt tip was used, and the effective tip radius was calibrated as $R = 310$ nm using a standard tungsten sample [20]. The tests were conducted in the continuous stiffness mode (CSM) [21], at a constant $\dot{P}/P = 0.05\ s^{-1}$, where P is the load. About 100 indents were performed at each condition for low uncertainty. The indents were separated by at least 20 μm to avoid interference.

Typical displacement-load curves that correspond to the average pop-in load are shown in Fig. 2a for the pristine and irradiated samples. Before pop-in, the load-displacement, P-h, curves fit well the Hertzian equation,

$$P = \frac{4}{3} E_r \sqrt{R} h^{3/2}, \tag{1}$$

where E_r is the reduced modulus, indicating a pure elastic response. As shown in the inset of Fig. 2a, pop-in load is very sensitive to irradiation damage, and is dropped by 70% after irradiation to the lowest fluence,

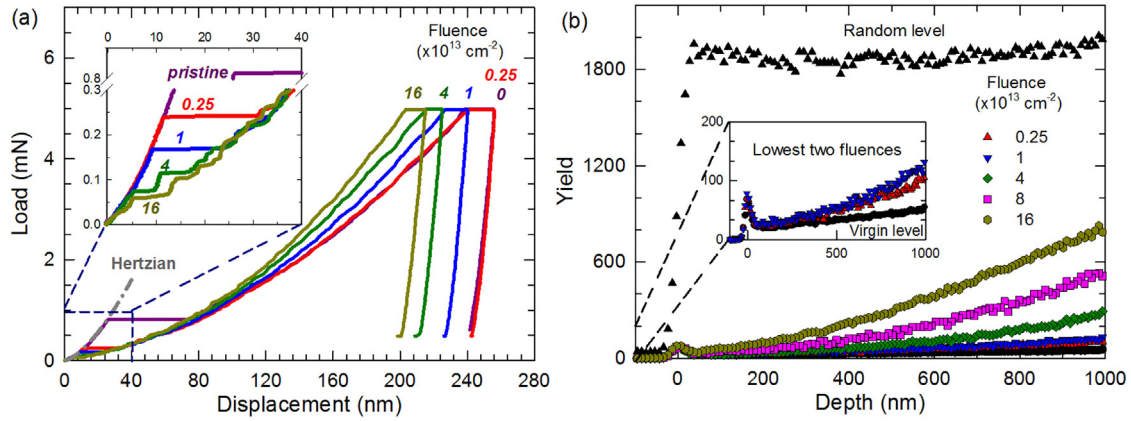

Fig. 2. Load-displacement curves and ion channeling spectra. (a) Typical load-displacement curves of Mo after irradiations with fluence from 2.5×10^{12} to 1.6×10^{14} cm^{-2}. Inset is the enlarged area with displacement below 40 nm. (b) RBS/C spectra of Mo from 2.5×10^{12} to 1.6×10^{14} cm^{-2}. Inset is enlarged for the lowest two fluences.

2.5×10^{12} cm^{-2}, corresponding to a surface dose of 7.5×10^{-4} dpa. With increasing irradiation fluence, pop-in load keeps decreasing gradually, and reaches the detection limit of ~0.05 mN (below 5 nm) after irradiations at 1.6×10^{14} cm^{-2}, corresponding to ~4.8×10^{-2} dpa. Such a rapid decrease in pop-in load probably caused the disappearance of pop-in after high dose (>0.5 dpa) irradiations [14, 15].

In contrast to the high sensitivity of pop-in load, ion channeling technique exhibits much weaker response to the low dose irradiations. As shown in Fig. 2b, the increase in backscattering yields is barely observable at the two lowest fluences (where the pop-in load drops most rapidly), due to its limited detection resolution on slight lattice distortion. The increase in channeling yield becomes more significant for higher doses (stronger lattice distortion), where the pop-in tests become insensitive.

To correlate the pop-in behavior to irradiation-induced defects, pop-in load is converted to the critical shear stress at pop-in, $\tau_{\max}$, of the material [22, 23] through

$$\tau_{\max} = 0.31 \times \left(\frac{6P_{pop-in}E_r^2}{\pi^3 R^2}\right)^{1/3}. \quad (2)$$

The cumulative pop-in probability, f_{total}, versus the shear strength of the material is shown in Fig. 3a (from 100 indentations with maximum load of 1.5 mN), which can be described by

$$f_{totat} = 1 - q_{hetero} \times q_{homo}. \quad (3)$$

Here q_{hetero} and q_{homo} represent the survivability from homogeneous and heterogeneous dislocation nucleation, respectively, and can be described by

$$q_{homo} = \exp\left(-\dot{n}_0 \int_0^{pop-in} \frac{dP}{\dot{P}} \int_\Omega \exp\left\{-\frac{\Delta\Pi(\tau_{shear})}{k_B T}\right\} d\Omega\right), \quad (4)$$

and

$$q_{hetero} = \exp\left(-\rho_{defect} V_d\right), \quad (5)$$

where $\dot{n}_0$ is the characteristic nucleation rates, k_B is the Boltzmann constant, T is the absolute temperature, $d\Omega$ is the differential volume, $\Delta\Pi(\tau_{shear})$ is the corresponding activation energy, ρ_{defect} is the density of heterogeneous dislocation nucleation sources (including the pre-existing sources prior to the irradiation such as Frank-Read sources, as well as the new sources generated by ion irradiation), and V_d is the stressed volume size in which shear stress is higher than the defect strength, τ_{defect}. Here defect strength is defined as the critical stress above which dislocations can be nucleated at the defect. The Eq. (4) is derived from thermally activated, homogeneous nucleation, and Eq. (5) is based on a weakest-link-type statistics for heterogeneous nucleation [9, 24]. There are only two fitting parameters in Eq. (4), being the characteristic nucleation rate and the activation energy, which are intrinsic and do not affect the heterogeneous nucleation sources. The fitting procedure and the corresponding fitting parameters have been elaborated in Ref. [20]. Eq. (5) models the activation of the heterogeneous dislocation nucleation sources, which is represented by the τ_{defect} and ρ_{defect}. These two parameters critically depend on the irradiation process and thus are key results of our work.

With increasing irradiation fluence, defect density increases, and pop-in occurs more readily through the heterogeneous mechanism since the stressed volume has a greater chance to contain nucleation sites. The derived density and strength of irradiation-induced defects are shown in Fig. 3b. The defect density increases rapidly in the low dose regime of 10^{-3} dpa, but much more slowly with further irradiations. This behavior qualitatively agrees with the previous TEM observations on neutron-irradiated Mo [25]. The activation stress of irradiation-induced defects decreases from ~0.42 to 0.24 τ_{th} (τ_{th} = 16.1 GPa) with increasing irradiation fluence, which are about one order magnitude higher than that obtained for both residual defects in as-prepared samples and the bulk samples after uniform compression tests, ~0.04 τ_{th} (derived by using large indenters that generate large stressed volumes, as reported in Ref. [20]). This finding indicates that the type of dislocation nucleation source induced from ion irradiations is qualitatively different from that induced by compression and sample preparation (e.g. deformation). During mechanical compression tests and sample preparation, dislocations in macroscopic length are introduced, and the heterogeneous nucleation source for pop-in has been believed mainly Frank-Read type that can be readily activated [20]. In contrast, low-dose irradiation in Mo introduces small interstitial-type loops less than a few nanometers in size, mono-vacancies and vacancy clusters [25, 26]. Such irradiation-induced defects also serve as local instabilities, but the stress needed for dislocation nucleation is much greater than that for Frank-Read sources.

Previous studies have reported that pre-existing vacancies or vacancy clusters can act as heterogeneous nucleation sites for dislocations [10, 13, 27]. Among these works, Salehinia et al. have quantitatively estimated the impact of several types of (point) defects on the stress needed for dislocation nucleation by molecular dynamics simulations [27]. The critical stress of dislocation nucleation can be reduced by up to 50% resulting from pre-existing point defects, which reasonably agrees with our observed defect strength. Such reduction has also been found enhanced with increasing cluster size (e.g. from 10, 20 to

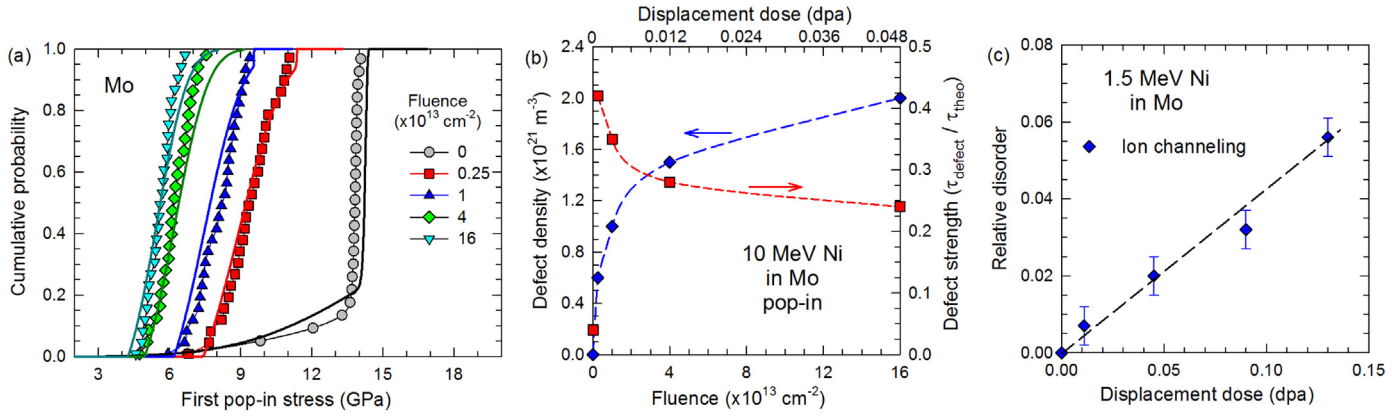

Fig. 3. Damage accumulation characterized from pop-in and ion channeling tests. (a) Cumulative pop-in probability versus the critical shear stress at pop-in. The symbols are the experimental results and the lines are the simulated curves using Eqs. (3)–(5). (b) Modeled density and strength of the irradiation-induced defects. (c) Relative disorder as a function of irradiation dose for Mo irradiated with 1.5 MeV Ni, from ion channeling analyses.

50% for mono-, di- and 55 vacancies, respectively), which might qualitatively explain our observation on the reduction of defect strength, since the average size of irradiation-induced defect clusters increases with increasing dose [25]. The impact of nm-size interstitial loops on the inception of plasticity is still unclear, which promotes a need for further atomistic simulations.

Ion channeling is performed as a complementary technique to characterize the irradiation induced overall lattice distortion. Lower energy (1.5 MeV) Ni ion irradiations were performed to achieve a shallower damage range (~850 nm) for proper data analysis. As shown in Fig. 3c, overall relative disorder is quantified as a function of irradiation dose in the range of 0.01–0.13 dpa at the damage peak of ~350 nm, using a iterative dechanneling analysis procedure [28].

The derived relative disorder from ion-channeling increases approximately linearly with increasing dose, which is different from what shown in Fig. 3b from pop-in tests. This discrepancy occurs since pop-in quantifies the density of defect clusters while ion channeling evaluates the overall lattice distortion. With increasing dose, overlap of collision cascades results in aggregation of small defect clusters, making the density deviated from linear increase [4]. The present results indicate a stronger dechanneling capability of a larger defect cluster than a smaller one during early stage damage accumulation.

Irradiation induced defects play two roles in nanoindentation tests. Locally, it produces the weakest links that trigger the heterogeneous dislocation nucleation, resulting in the reduction of pop-in load. At the bulk limit, they serve as obstacles of dislocation migration, causing strain-hardening. The depth-dependent nanoindentation hardness is shown in Fig. 4a, in which the values below 85 nm are omitted due to the pop-in and surface artificial. The size effects are significant in the pristine Mo, which can be reasonably fit by the Nix-Gao model [29], as shown in the inset of Fig. 4a,

$$H^2 = H_0^2(1 + h^*/h), \tag{6}$$

where H_0 is the hardness in the limit of infinite depth and h^* is a characteristic length that depends on the shape of the indenter. After irradiations, especially when the fluence reaches 1×10^{13} cm^{-2}, the size effects are much weaker and are only significant in the first tens of nanometers (omitted here). After correcting size effects, the hardness change as a function of irradiation fluence is shown in Fig. 4b, which can be described by

$$\Delta H = A[1 - \exp(-BD)]^C, \tag{7}$$

where D is the dose or fluence; and A, B, and C are fitting parameters. The exponential term in Eq. (7) comes from the saturation in defect density in the process of damage accumulation [30, 31]. The fitted parameter values are 1.59, 0.18, and 0.44 for A, B, and C, respectively, when GPa and 10^{13} cm^{-2} are used as the units of indentation hardness H and fluence D.

Taylor strengthening has been widely used to describe irradiation induced hardening [32] as

$$\Delta H \propto \Delta\sigma_y = \alpha M G b\sqrt{\rho_{def} d}, \tag{8}$$

where M is the Taylor factor, ~3 for body-centered cubic lattice, α is a material dependent constant, G is the shear modulus, b is the Burgers vector, and d is the defect size. The hardness measurement itself can only provide the product of defect size and density as a function of irradiation fluence. However, combined with the defect density information from pop-in test, the evolution of defect size can be qualitatively derived. Note that the absolute value of defect size cannot be derived since the absolute value of α is unknown. As shown in Fig. 4c, the average defect size increases with increasing irradiation fluence with a declining growth rate, consistent with the literature results [25], and provides an evidence to our suggested origin of the decrease in defect strength. Such agreements indicate that the characterization of defect production and evolution using nanoindentation pop-in and hardness tests are self-consistent and realistic. It needs to be noted that although surface condition may be modified by ion irradiation, which may result in uncertainties for pop-in tests, the present study is in the very low dose regime and therefore such uncertainties are expected to be small. Furthermore, the present study only provides the averaged results in the region of interest, although the local dose only varies to a small extent; further depth-resolved characterizations are desired.

In the present study, nanoindentation pop-in tests have been demonstrated as an effective quantitative method to study the early stage damage accumulation induced by low-fluence ion irradiations. The irradiation-induced defects in single crystalline Mo significantly reduce the pop-in load. The defect production and evolution as a function of irradiation fluence have been derived using a unified model convoluting homogeneous and heterogeneous dislocation nucleation mechanisms. Unlike ion channeling technique, nanoindentation tests can separate the effects of evolving density and size of defects. Defect density increases more rapidly in the lower dose regime. The strength of irradiation-induced defects is one order magnitude higher than the Frank-Read sources induced from mechanical straining, and decreases with increasing irradiation dose, attributed to the growth of defect

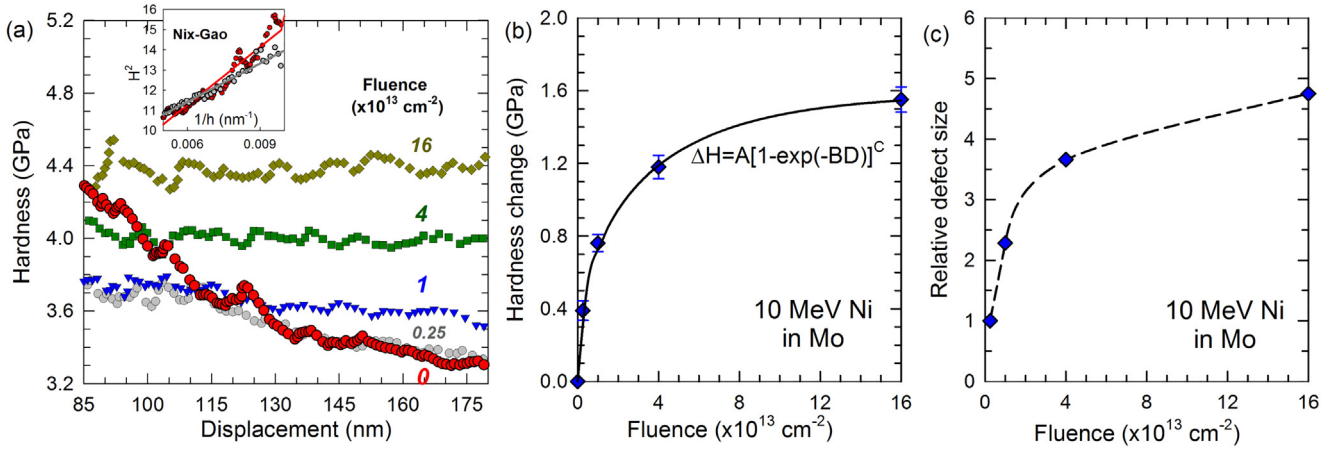

Fig. 4. Irradiation induced hardening and defect size evolution. (a) Nanoindentation hardness as a function of depth after irradiations to different doses. Inset shows the Nix-Gao size effect relationship in the pristine sample and that irradiated at the lowest fluence. (b) Change in nanoindentation hardness as a function of irradiation fluence. (c) Relative defect size as function of irradiation fluence (normalized to the value at 2.5×10^{12} cm^{-2}).

clusters. To this end, combining ion irradiation and pop-in tests may further be used as a unique method to study the effects of point defect clusters on the incipient plasticity of materials.

Acknowledgements

This work was supported as part of the Energy Dissipation to Defect Evolution (EDDE), an Energy Frontier Research Center funded by the U.S. Department of Energy, Office of Science, Basic Energy Sciences. Work of YFG (statistic model) was supported by the U.S. Department of Energy, Office of Science, Basic Energy Sciences, Materials Sciences and Engineering Division. Ion beam works were performed at the UT–ORNL Ion Beam Materials Laboratory (IBML) located at the campus of the University of Tennessee, Knoxville.

References

[1] S.J. Zinkle, G.S. Was, Acta Mater. 61 (2013) 735.
[2] S. Duzellier, Aerosp. Sci. Technol. 9 (2005) 93.
[3] G.S. Was, Fundamentals of Radiation Materials Science: Metals and Alloys, Springer, Berlin, Heidelberg, New York, 2007.
[4] B.N. Singh, S.J. Zinkle, J. Nucl. Mater. 206 (1993) 212.
[5] C.P. Race, D.R. Mason, M.W. Finnis, W.M.C. Foulkes, A.P. Horsfield, A.P. Sutton, Rep. Prog. Phys. 73 (2010) 116501.
[6] Y. Zhang, G.M. Stocks, K. Jin, C. Lu, H. Bei, B.C. Sales, L. Wang, L.K. Beland, R.E. Stoller, G.D. Samolyuk, M. Caro, A. Caro, W.J. Weber, Nat. Commun. 6 (2015) 8736.
[7] Y. Zhang, S. Zhao, W.J. Weber, K. Nordlund, F. Granberg, F. Djurabekova, Curr. Opin. Solid State Mater. Sci. 21 (2017) 221.
[8] R.S. Averback, R. Benedek, K.L. Merkle, Phys. Rev. B 18 (1978) 4156.
[9] Y. Gao, H. Bei, Prog. Mater. Sci. 82 (2016) 118.
[10] C.A. Schuh, J.K. Mason, A.C. Lund, Nat. Mater. 4 (2005) 617.
[11] R. Abram, D. Chrobak, R. Nowak, Phys. Rev. Lett. 118 (2017), 095502.
[12] L. Zhang, T. Ohmura, Phys. Rev. Lett. 112 (2014) 145504.
[13] J.K. Mason, A.C. Lund, C.A. Schuh, Phys. Rev. B 73 (2006), 054102.
[14] A.J. Bushby, S.G. Roberts, C.D. Hardie, J. Mater. Res. 27 (2011) 85.
[15] S. Pathak, S.R. Kalidindi, J.S. Weaver, Y. Wang, R.P. Doerner, N.A. Mara, Sci. Rep. 7 (2017).
[16] L.C. Feldman, J.W. Mayer, S.T. Picraux, Materials Analysis by Ion Channeling, Academic Press, 1982.
[17] Y. Zhang, M.L. Crespillo, H. Xue, K. Jin, C.H. Chen, C.L. Fontana, J.T. Graham, W.J. Weber, Nucl. Instrum. Methods B 338 (2014) 19.
[18] J.F. Ziegler, in www.srim.org.
[19] C.H.M. Broeders, A.Y. Konobeyev, J. Nucl. Mater. 328 (2004) 197.
[20] H. Bei, Y.Z. Xia, R.I. Barabash, Y.F. Gao, Scr. Mater. 110 (2016) 48.
[21] W.C. Oliver, G.M. Pharr, J. Mater. Res. 7 (1992) 1564.
[22] K.L. Johnson, Contact Mechanics, Cambridge University Press, Cambridge, 1985.
[23] H. Bei, Y.F. Gao, S. Shim, E.P. George, G.M. Pharr, Phys. Rev. B 77 (2008).
[24] J.R. Morris, H. Bei, G.M. Pharr, E.P. George, Phys. Rev. Lett. 106 (2011) 165502.
[25] M. Li, M. Eldrup, T.S. Byun, N. Hashimoto, L.L. Snead, S.J. Zinkle, J. Nucl. Mater. 376 (2008) 11.
[26] B.N. Singh, J.H. Evans, A. Horsewell, P. Toft, G.V. Muller, J. Nucl. Mater. 258–263 (1998) 865.
[27] I. Salehinia, D.F. Bahr, Scr. Mater. 66 (2012) 339.
[28] Y. Zhang, J. Lian, Z. Zhu, W.D. Bennett, L.V. Saraf, J.L. Rausch, C.A. Hendricks, R.C. Ewing, W.J. Weber, J. Nucl. Mater. 389 (2009) 303.
[29] W.D. Nix, H. Gao, J. Mech. Phys. Solids 46 (1998) 411.
[30] W.J. Weber, J. Nucl. Mater. 98 (1981) 206.
[31] W.J. Weber, E. Wendler, in: W. Wesch, E. Wendler (Eds.), Ion Beam Modification of Solids, Springer International Publishing Switzerland 2016, pp. 105–136.
[32] G.E. Lucas, J. Nucl. Mater. 206 (1993) 287.